

**Nucleon form factors and final state radiative corrections to  $e^+e^- \rightarrow \bar{p}p\gamma$** Henryk Czyż,<sup>1</sup> Johann H. Kühn,<sup>2</sup> and Szymon Tracz<sup>1</sup><sup>1</sup>*Institute of Physics, University of Silesia, PL-40007 Katowice, Poland*<sup>2</sup>*Institut für Theoretische Teilchenphysik, Karlsruhe Institute of Technology, D-76128 Karlsruhe, Germany*

(Received 31 July 2014; published 16 December 2014)

New parametrizations for the electric and the magnetic form factors of a proton and neutron are presented. The proton form factors describe well the recent measurements by the *BABAR* Collaboration and earlier ones of the ratio of the form factors in a spacelike region. The neutron form factors are consistent with earlier measurements of neutron pair production and ratio of the form factors in the spacelike region. These form factors are implemented into the generator PHOKHARA, which simulates the reactions  $e^+e^- \rightarrow \bar{p}p\gamma$  and  $e^+e^- \rightarrow \bar{n}n\gamma$ . The influence of final state radiation is investigated.

DOI: 10.1103/PhysRevD.90.114021

PACS numbers: 13.66.Bc, 13.40.Gp

**I. INTRODUCTION**

Nucleon form factors both in the spacelike and in the timelike regions have attracted theoretical as well as experimental attention from the early times of particle physics [1–4]. Experiments for electron-proton scattering give access to the spacelike region, and detailed analyses of angular distributions without [2] and with [5] a polarized beam and target allow us to separate the magnetic and electric form factors. The cross section for proton-antiproton production at electron-positron colliders (or the inverse reaction  $p\bar{p} \rightarrow e^+e^-$ ) gives access to a specific combination of form factors in the timelike region. The additional analysis of angular distributions allows us to separate magnetic and electric form factors. Recently, discrepancies have been found between the ratio of magnetic and electric form factors extracted in the spacelike region using the Rosenbluth method or, alternatively, using a polarized beam and/or target (see [6] for a review). The mentioned inconsistency was, to a large extent, explained theoretically by enhanced contributions from two-photon exchange (see [7] for a review). Nevertheless, this has triggered a new experiment (OLYMPUS) [8] to measure both electron and positron scattering off protons and designed to resolve this issue experimentally. Form factors in the spacelike and timelike regions are connected via analyticity. Thus, measurements in  $e^+e^-$  collisions may help to resolve this issue. Even more important, these measurements are ideally suited to search for baryon-antibaryon resonances close to production threshold as well as at higher energies. Last but not least, the high energy behavior has been predicted in the framework of perturbative QCD [9], predictions that could be checked at high energy. For recent reviews on nucleon electromagnetic form factors, we refer the reader to [10,11].

There are three reactions that are currently used for measurements in the timelike region:  $e^+e^- \rightarrow p\bar{p}$ ,  $p\bar{p} \rightarrow e^+e^-$ , and the radiative return reaction  $e^+e^- \rightarrow p\bar{p}\gamma$ . Given sufficiently large luminosity, the third

reaction allows us to measure the form factors in principle from threshold up to the collider energy. The radiative return has been employed successfully by the *BABAR* experiment [12], which has measured the production rate and the ratio of the form factors with a precision of 7% and 11%, respectively. In view of this improvement, we present a parametrization of the nucleon form factors, which is based on generalized vector dominance, similar to that from [13] for the case of pion and kaon pair production. Furthermore, we consider in detail the impact of final state radiation to this measurement. In our simplified model, we treat real radiation similar to the radiation from a pointlike particle. As far as the virtual corrections are concerned, we include the Coulomb enhancement factor, important close to threshold and an infrared subtraction term to compensate for soft real radiation. These ingredients are implemented into Monte Carlo event generator PHOKHARA version 9.1, and the effect of these modifications is studied in detail. Additionally, the same modifications are added to the description of proton-antiproton pair production in the scanning mode ( $e^+e^- \rightarrow p\bar{p}$ ) in PHOKHARA version 9.1.

**II. NUCLEON FORM FACTORS**

In the first implementation [14] of nucleon pair production through the radiative return ( $e^+e^- \rightarrow \bar{N}N\gamma$ ) into the event generator PHOKHARA a model of the nucleon form factors was used, which had been taken from [15]. To accommodate the experimental data, which are available now, we propose a new improved model for the Dirac and Pauli nucleon form factors

$$F_{1,2}^p = F_{1,2}^s + F_{1,2}^v, \quad (1)$$

$$F_{1,2}^n = F_{1,2}^s - F_{1,2}^v, \quad (2)$$

which enter the electromagnetic current

$$J_\mu = -ie\bar{v}(p_2) \left( F_1^N(Q^2)\gamma_\mu - \frac{F_2^N(Q^2)}{4m_N} [\gamma_\mu, \not{Q}] \right) u(p_1), \quad (3)$$

where  $Q = p_1 + p_2$ . The indices  $s$  and  $v$  refer to isospin zero and one, respectively.

We use the following ansatz:

$$F_1^s = \frac{1}{2} \frac{\sum_{n=0}^4 c_n^1 BW_{\omega_n}(s)}{\sum_{n=0}^4 c_n^1}, \quad (4)$$

$$F_1^v = \frac{1}{2} \frac{\sum_{n=0}^4 c_n^2 BW_{\rho_n}(s)}{\sum_{n=0}^4 c_n^2}, \quad (5)$$

$$F_2^s = -\frac{1}{2} b \frac{\sum_{n=0}^4 c_n^3 BW_{\omega_n}(s)}{\sum_{n=0}^4 c_n^3}, \quad (6)$$

$$F_2^v = \frac{1}{2} a \frac{\sum_{n=0}^4 c_n^4 BW_{\rho_n}(s)}{\sum_{n=0}^4 c_n^4}, \quad (7)$$

where  $c_0^i = 1$  for  $i = 1, 2, 3, 4$ . Following the Zweig rule, we neglect the  $\phi$  contributions. The Breit-Wigner function is defined as

$$BW_i(Q^2) = \frac{m_i^2}{m_i^2 - Q^2 - im_i\Gamma_i\theta(Q^2)}. \quad (8)$$

The step function  $\theta(Q^2)$  sets the mesons' widths to zero for spacelike  $Q^2$ . Above the proton-antiproton production threshold, we use constant meson widths. The normalization of electric and magnetic form factors in the limit of  $s = 0$  to electric charges and magnetic moments of nucleons fixes the parameters  $a = \mu_p - \mu_n - 1$  and  $b = -\mu_p - \mu_n + 1$ , where  $\mu_p(\mu_n)$  are the magnetic moments of the proton (neutron). We impose the asymptotic (large  $Q^2$ ) behavior of the form factors predicted in perturbative QCD [9]

$$F_1 \sim \frac{1}{(Q^2)^2}, \quad F_2 \sim \frac{1}{(Q^2)^3}, \quad (9)$$

which leaves six independent complex parameters to be determined by experimental data. Below we rewrite them using real parameters  $c_i^j = c_i^{jR} + ic_i^{jI}\theta(Q^2)$ .

The asymptotic behavior Eq. (9) is enforced by choosing

$$c_4^1 = -\frac{1}{m_{\omega_4}^2} \sum_{n=0}^3 m_{\omega_n}^2 c_n^1, \quad (10)$$

$$c_4^2 = -\frac{1}{m_{\rho_4}^2} \sum_{n=0}^3 m_{\rho_n}^2 c_n^2, \quad (11)$$

$$c_3^3 = \frac{\sum_{n=0}^2 m_{\omega_n}^2 c_n^3 (m_{\omega_n}^2 - m_{\omega_4}^2 + i(m_{\omega_4}\Gamma_{\omega_4} - m_{\omega_n}\Gamma_{\omega_n}))}{m_{\omega_3}^2 (m_{\omega_4}^2 - m_{\omega_3}^2 + i(m_{\omega_3}\Gamma_{\omega_3} - m_{\omega_4}\Gamma_{\omega_4}))},$$

$$c_4^3 = -\frac{1}{m_{\omega_4}^2} \sum_{n=0}^3 m_{\omega_n}^2 c_n^3, \quad (12)$$

$$c_3^4 = \frac{\sum_{n=0}^2 m_{\rho_n}^2 c_n^4 (m_{\rho_n}^2 - m_{\rho_4}^2 + i(m_{\rho_4}\Gamma_{\rho_4} - m_{\rho_n}\Gamma_{\rho_n}))}{m_{\rho_3}^2 (m_{\rho_4}^2 - m_{\rho_3}^2 + i(m_{\rho_3}\Gamma_{\rho_3} - m_{\rho_4}\Gamma_{\rho_4}))}, \quad (13)$$

$$c_4^4 = -\frac{1}{m_{\rho_4}^2} \sum_{n=0}^3 m_{\rho_n}^2 c_n^4. \quad (14)$$

The Dirac and Pauli form factors for each nucleon  $N$  are related to the electric  $G_E^N$  and magnetic  $G_M^N$  through ( $\tau = Q^2/4m_N^2$ ),

$$G_E^N = F_1^N + \tau F_2^N, \quad (15)$$

$$G_M^N = F_1^N + F_2^N. \quad (16)$$

The masses and widths of the mesons and nucleons were taken from the Particle Data Group [16] with the exception of  $\rho_{3,4}$  and  $\omega_{3,4}$  adopted from kaon form factor model [13] ( $m_{\rho_3} = 2.12$  GeV,  $\Gamma_{\rho_3} = 0.3$  GeV,  $m_{\omega_3} = 2.0707$  GeV,  $\Gamma_{\omega_3} = 1.03535$  GeV,  $m_{\rho_4} = 2.32647$  GeV,  $\Gamma_{\rho_4} = 0.4473$  GeV,  $m_{\omega_4} = 2.34795$  GeV,  $\Gamma_{\omega_4} = 1.173975$  GeV). The model parameters, namely, the complex  $V\bar{N}N$  couplings, were fitted to the following experimental data:  $e^+e^- \rightarrow \bar{p}p$  cross section [12,17–23],  $\bar{p}p \rightarrow e^+e^-$  cross section [24–29],  $e^+e^- \rightarrow \bar{n}n$  cross section [21], ratio of the proton electric and magnetic form factors in the spacelike [30–33] and timelike [12,24] regions, and ratio of the neutron electric and magnetic form factors in the spacelike region [34,35]. The cross sections of the reaction  $ep \rightarrow ep$ , which depend also on the form factors we model, contain also non-negligible contributions from two-photon exchange diagrams [7]. The modeling of these contributions is beyond the scope of this paper, and we adopted the following procedure to get a reasonable description of this cross section as well: We consider only one data set [36] covering a large range of angles and kinematical invariant ( $Q^2$ ). In fit, we neglect the contribution from two-photon exchange diagrams, and to account for this, we enlarge the cross section error bars used in the fitting procedure to 10% of the cross section.

A fit to all the above experimental data leads to unacceptable results ( $\chi^2 = 214$  for 177 data points). The reason is that the PS170 [24–26] and DM2 [17,18] data are in conflict with the BABAR data [12]. It is quite implausible that any model can accommodate PS170 and BABAR data sets at the same time, as the ratio of the form factors is in evident conflict and, even more important, both  $e^+e^- \rightarrow \bar{p}p$  and  $\bar{p}p \rightarrow e^+e^-$  cross sections are proportional to the same combination of the magnetic and electric form factors

TABLE I. Values of the chi-squared distribution for particular experiments: number of experimental points (nep), cross section (cs), ratio of the electric and magnetic form factors (r). The PS170 and DM2 data were excluded from this fit (see text for details).

Experiment	nep	$\chi^2$	Experiment	nep	$\chi^2$
<i>BABAR</i> cs [12]	38	30	<i>BABAR</i> r [12]	6	0.6
PS170 <sub>1</sub> cs [24]	8	109	PS170 r [24]	5	16
PS170 <sub>2</sub> cs [25]	4	4	PS170 <sub>3</sub> cs [26]	4	52
E760 <sub>1</sub> cs [27]	3	0.5	E835 <sub>1</sub> cs [28]	5	1
E835 <sub>2</sub> cs [29]	2	0.03	DM2 cs [17,18]	7	26
BES cs [19]	8	10	CLEO cs [20]	1	0.4
FENICE cs [21]	5	5	DM1 cs [22]	4	0.7
JLab 05 r [30]	10	16	JLab 02 r [31]	4	1
JLab 01 r [32]	13	10	JLab 10 r [33]	3	6
MAMI 01 r [37]	3	2	JLab 03 r [34]	3	6
BLAST 08 r [35]	4	6	FENICE cs [21]	4	0.6
			SLAC cs [36]	32	27

TABLE II. Parameters of the nucleons form factor for the fit, where the PS170 and DM2 data were excluded (see text for details).

$c_1^{1R}$	-0.45(1)	$c_1^{1I}$	-0.54(2)	$c_1^{2R}$	-0.27(1)	$c_2^{1I}$	0.18(1)
$c_3^{1R}$	0.42(2)	$c_3^{1I}$	0.37(2)	$c_1^{2R}$	-0.12(1)	$c_2^{2I}$	-3.06(2)
$c_2^{2R}$	0.16(1)	$c_2^{2I}$	2.53(1)	$c_3^{2R}$	-0.32(1)	$c_3^{2I}$	-0.17(1)
$c_3^{2R}$	-8.03(5)	$c_3^{2I}$	3.28(2)	$c_2^{3R}$	10.6(1)	$c_2^{3I}$	0.2(3)
$c_1^{4R}$	-0.845(1)	$c_1^{4I}$	0.364(1)	$c_2^{4R}$	0.427(1)	$c_2^{4I}$	-0.305(1)

( $|G_M^p|^2(1 + \cos^2\theta) + \frac{|G_E^p|^2}{\tau} \sin^2\theta$ ) (where  $\theta$  is the scattering angle), and, thus, the same function is measured in both cases.

The model accommodates well the whole data set if one excludes either PS170 and DM2 ( $\chi^2 = 124$  for 150 data points) or *BABAR* data ( $\chi^2 = 107$  for 133 data points). In both cases, the  $\chi^2$  values are excellent, but each of the models is in strong conflict with the data set which was not fitted. We report here only the details of the fit (Tables I and II, Figs. 1–5), where PS170 and DM2 data were excluded. Nevertheless, it would be highly desirable to confirm the *BABAR* data by an independent measurement with similar precision. One observes (Fig. 4) that for model building, a more accurate neutron-antineutron cross section would be desirable, as the presently available data give little constraints on the model parameters.

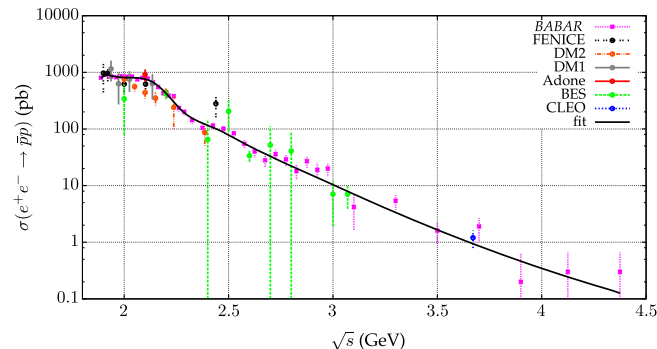


FIG. 1 (color online). The experimental data compared to the model fits results.

### III. FINAL STATE RADIATION (FSR) CORRECTIONS TO $e^+e^- \rightarrow \bar{p}p\gamma$

The *BABAR* data set was obtained with the radiative return method, and final state photon(s) emission was argued to be negligible [12]. As an independent data set

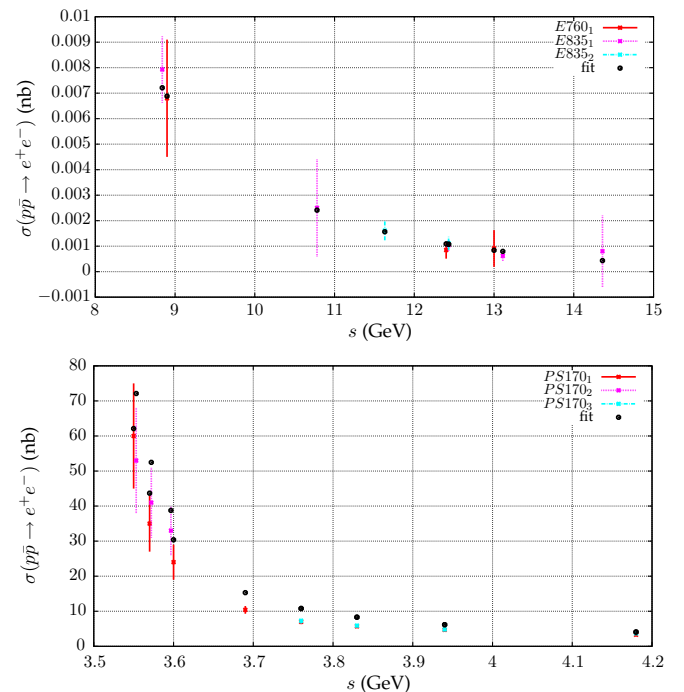


FIG. 2 (color online). The experimental data compared to the model fits results.

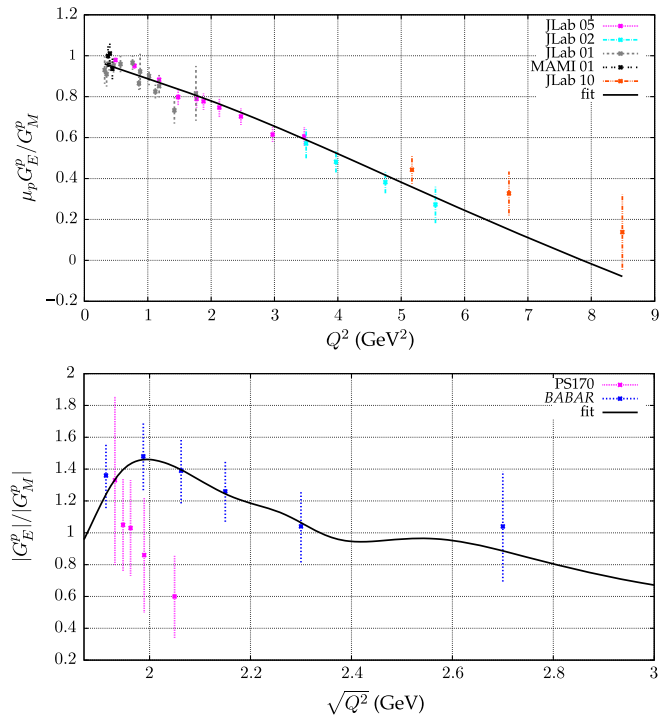


FIG. 3 (color online). The experimental data compared to the model fits results. Ratio of the electric and magnetic proton form factors in spacelike (upper plot) and timelike (lower plot) regions.

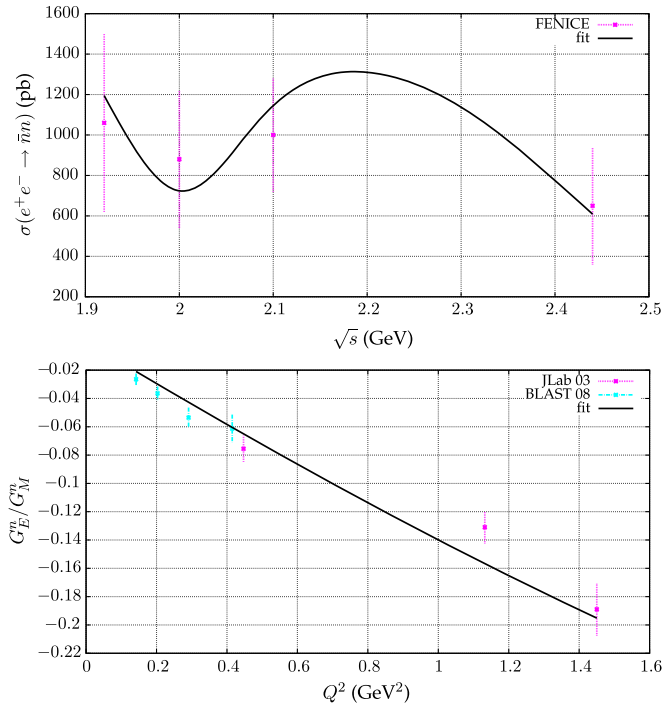


FIG. 4 (color online). The experimental data compared to the model fits results. Neutron-antineutron production cross section (upper plot) and ratio of the electric and magnetic neutron form factors in the spacelike region (lower plot).

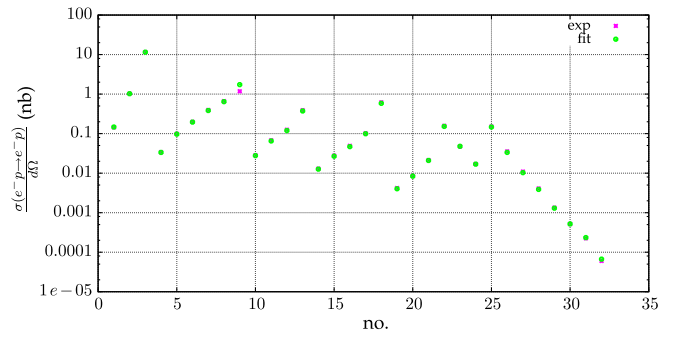


FIG. 5 (color online). The experimental data [36] compared to the model fit results. The data points and fit results are overlaid for most cases. On the horizontal axis, the entry number from Table IV of [36] is given.

might be obtained, for example, via radiative return method with higher accuracy, the role of final state emission has to be reconsidered. As evident from the previous section, photon-nucleon interactions are not well known. Modeling of real photon emission from a proton is, thus, difficult. We follow here the scheme adopted successfully in [38] for final state emission from charged pions. For the proton, the situation is more complicated due to the presence of the Pauli form factor at leading order, and the model is not renormalizable. Here we adopted the simplest model assuming that real photon emission from a proton (antiproton) looks like emission from a pointlike charged particle. This means that it is identical to the emission from muons [39]. For the virtual corrections, one cannot simply adapt the corrections from the muon case. Because of the presence of the  $F_2$  form factor, they are not the same, and the corrections proportional to  $F_1$  and  $F_2$  are not expected to be identical. Moreover, as the theory based on the interaction Lagrangian  $\mathcal{L} = A^\mu J_\mu$ , with  $A_\mu$  being the electromagnetic field and  $J_\mu$  defined in Eq. (3), is not renormalizable, further complications arise. They will not be addressed in this paper. For the virtual corrections, we have used an overall factor, multiplying zero-, one-, and two-photon emission parts:

$$C(Q^2) = f(\pi\alpha/\beta) - f(\pi\alpha) + 1, \quad (17)$$

where

$$f(x) = \frac{x}{1 - \exp(-x)}, \quad \beta = \sqrt{1 - 4m_p^2/Q^2}, \quad (18)$$

$m_p$  is the proton mass, and  $Q^2$  is the invariant mass of proton-antiproton pair.

At small proton velocities,  $C(Q^2)$  reproduces the usual Coulomb factor which resums the leading radiative corrections for small velocities, while at large invariant masses,  $C(Q^2 \rightarrow \infty) \rightarrow 1$ . In addition, a correction of the form

$$\Delta_{\text{final}} = \frac{2\alpha}{\pi} \left[ \frac{(1 + \beta^2)}{2\beta} \log \frac{Q^2(1 + \beta)^2}{4m_p^2} - 1 \right] \log 2w \quad (19)$$

with  $w = E_{\gamma,\text{min}}/\sqrt{s}$  was added, where  $E_{\gamma,\text{min}}$  is a separation parameter between the soft and hard parts of the photon phase space. It compensates the divergences arising from integration of a real emitted photon with energy  $E_\gamma > E_{\gamma,\text{min}}$ . Technically, it leads to the replacement of  $\frac{\alpha}{\pi} \eta^{V+S}$  used for muons in [39] with  $\Delta_{\text{final}}$ . The factor  $C$  takes care of the proper threshold behavior. Both  $C$  and  $\Delta_{\text{final}}$  factors are generic for any model, which assumes that for soft photon emission, the proton behaves like a pointlike particle. In any more elaborated model for the virtual corrections, there will be additional finite corrections proportional to  $\alpha/\pi$ , which will depend on the model details. In our ansatz, we put them to zero. They are not expected to be big, and their size can be tested using charge asymmetries as proposed in [38,40,41] for pion pair production. In our opinion, without experimental tests of the FSR corrections, better modeling of these contributions is not possible.

The size of the FSR radiative corrections depends both on the energy of an experiment and on the event selection used and can be both negative or positive. In Fig. 6 we show its size for an event selection close to the one used by *BABAR*. We show there a relative difference of the ISR

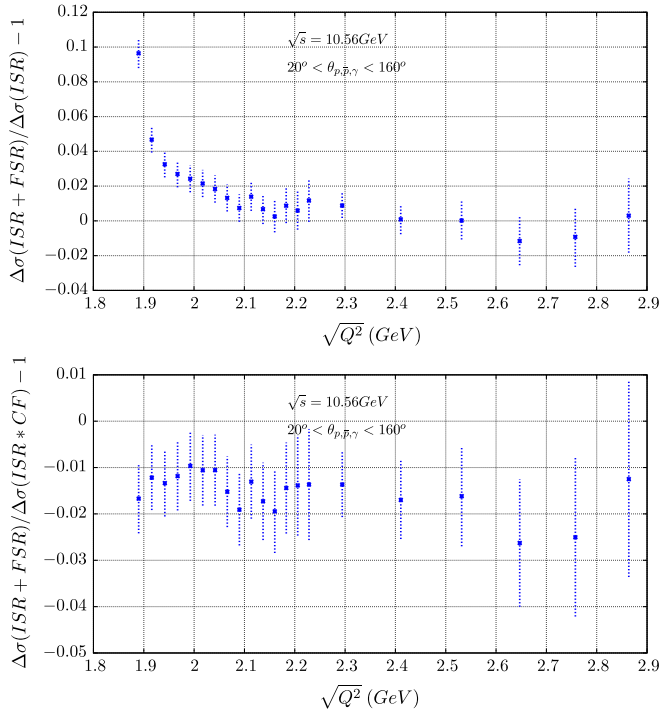


FIG. 6 (color online). Relative difference between  $Q^2$  distributions calculated at NLO with and without FSR radiative corrections and between complete FSR corrections and FSR corrections where only the Coulomb factor is included.

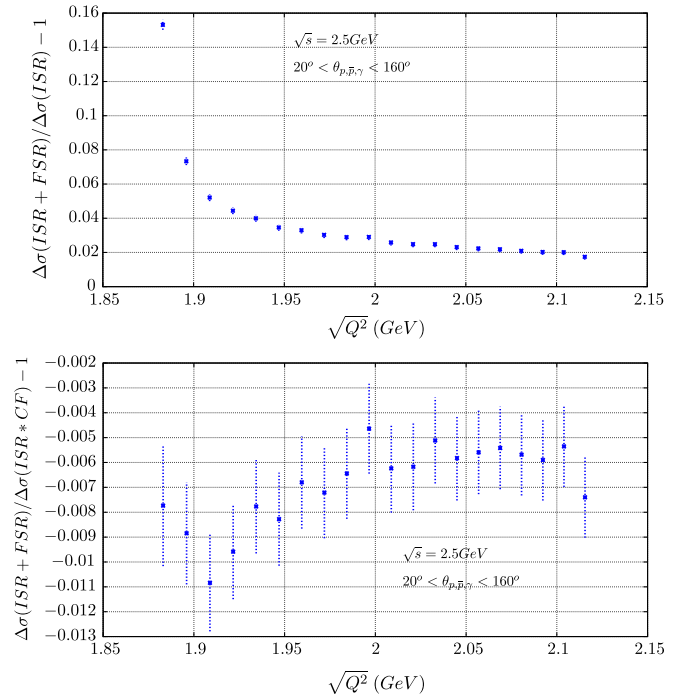


FIG. 7 (color online). Relative difference between  $Q^2$  distributions calculated at NLO with and without FSR radiative corrections and between complete FSR corrections and FSR corrections where only the Coulomb factor is included.

cross section calculated at next-to-leading order (NLO) and the initial state radiation (ISR) cross section corrected with Coulomb factor

$$C_F(Q^2) = f(\pi\alpha/\beta). \quad (20)$$

The difference between the FSR correction calculated with Coulomb factor only and FSR at NLO is also shown in Fig. 6. Its typical size is of order 1%. In Fig. 7 we show the same differences calculated at a possible BES III energy. The FSR corrections not included in the Coulomb factor  $C_F(Q^2)$  are here even lower than at *BABAR* energy, but still of order of 1% at low proton-antiproton pair invariant masses. As the FSR corrections for proton-antiproton pair production were not tested experimentally, the 1% contribution coming from our model should be taken conservatively as an estimate of the accuracy of the modeling of the FSR.

FSR corrections were also implemented for the proton-antiproton final state in the “scan” mode of the PHOKHARA Monte Carlo event generator [42]. Only the Coulomb factor Eq. (20) was taken into account. Its size is demonstrated in Fig. 8. From this figure, one can see that in any scan experiment in the region close to the threshold where, in principle, one can test the resummation of radiative corrections, the beam energy smearing effects (where the beam spread is typically 1–2 MeV) will obscure the effect. The distance between the first two points is taken as

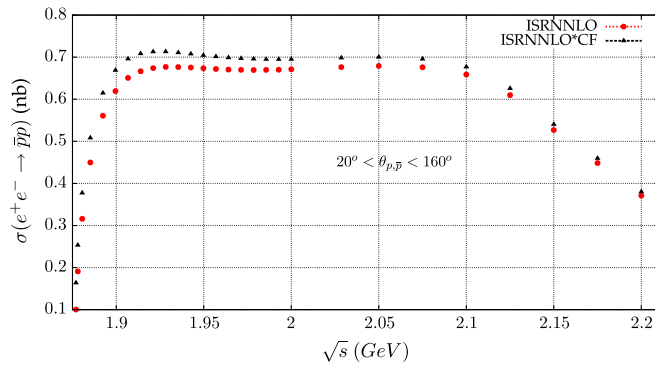


FIG. 8 (color online). The cross section of the reaction  $e^+e^- \rightarrow \bar{p}p$  with ISR at next-to-next-to-leading-order corrections included is compared to the same cross section where, in addition, FSR Coulomb corrections were added.

1.5 MeV, while between the second and the third point, the step size is 2 MeV.

The event generator PHOKHARA 9.1, which includes the new nucleon form factors and final state corrections is available on the PHOKHARA web page [43]. The newly added part of the code proportional to the Pauli form factor with real photon emission was tested using an independently written code. In the distributed code, the helicity amplitude method is used. Tests on the independence of the cross section on the soft-hard photon separation parameter

were also performed with the accuracy not worse than 0.03%.

#### IV. CONCLUSIONS

We have constructed nucleon form factors on the basis of generalized vector dominance which are consistent with recent *BABAR* results for proton-antiproton production through the radiative return, with older data for neutron-antineutron production and with results for electron-nucleon scattering. Furthermore, these form factors exhibit the high energy behavior predicted from perturbative QCD. We have considered the effect of final state radiation, demonstrating its smallness for typical experimental cuts. The new form factors and real as well as virtual final state radiation have been implemented in the Monte Carlo generator PHOKHARA.

#### ACKNOWLEDGMENTS

This work was supported in part by the Polish National Science Centre, Grant No. DEC-2012/07/B/ST2/03867 and German Research Foundation DFG under Contract No. Collaborative Research Center CRC-1044. H.C. is grateful for the support and the kind hospitality of the Institut für Theoretische Teilchenphysik of the Karlsruhe Institute of Technology.

- 
- [1] I. Estermann, R. Frisch, and O. Stern, *Nature (London)* **132**, 169 (1933).
- [2] M. Rosenbluth, *Phys. Rev.* **79**, 615 (1950).
- [3] R. Mcallister and R. Hofstadter, *Phys. Rev.* **102**, 851 (1956).
- [4] R. Hofstadter, *Rev. Mod. Phys.* **28**, 214 (1956).
- [5] A. I. Akhiezer and M. P. Rekalov, *Sov. Phys. Dokl.* **13**, 572 (1968).
- [6] J. Arrington, *Phys. Rev. C* **68**, 034325 (2003).
- [7] C. E. Carlson and M. Vanderhaeghen, *Annu. Rev. Nucl. Part. Sci.* **57**, 171 (2007).
- [8] R. Milner *et al.* (OLYMPUS Collaboration), *Nucl. Instrum. Methods Phys. Res., Sect. A* **741**, 1 (2014).
- [9] G. P. Lepage and S. J. Brodsky, *Phys. Rev. D* **22**, 2157 (1980).
- [10] C. Perdrisat, V. Punjabi, and M. Vanderhaeghen, *Prog. Part. Nucl. Phys.* **59**, 694 (2007).
- [11] A. Denig and G. Salme, *Prog. Part. Nucl. Phys.* **68**, 113 (2013).
- [12] J. Lees *et al.* (*BABAR* Collaboration), *Phys. Rev. D* **87**, 092005 (2013).
- [13] H. Czyz, A. Grzelinska, and J. H. Kuhn, *Phys. Rev. D* **81**, 094014 (2010).
- [14] H. Czyz, J. H. Kuhn, E. Nowak, and G. Rodrigo, *Eur. Phys. J. C* **35**, 527 (2004).
- [15] F. Iachello, A. Jackson, and A. Lande, *Phys. Lett.* **43B**, 191 (1973).
- [16] J. Beringer *et al.* (Particle Data Group), *Phys. Rev. D* **86**, 010001 (2012).
- [17] D. Bisello, S. Limentani, M. Nigro, L. Pescara, M. Posocco *et al.*, *Nucl. Phys.* **B224**, 379 (1983).
- [18] D. Bisello *et al.* (DM2 Collaboration), *Z. Phys. C* **48**, 23 (1990).
- [19] M. Ablikim *et al.* (BES Collaboration), *Phys. Lett. B* **630**, 14 (2005).
- [20] T. Pedlar *et al.* (CLEO Collaboration), *Phys. Rev. Lett.* **95**, 261803 (2005).
- [21] A. Antonelli, R. Baldini, P. Benasi, M. Bertani, M. Biagini *et al.*, *Nucl. Phys.* **B517**, 3 (1998).
- [22] B. Delcourt, I. Derado, J. Bertrand, D. Bisello, J. Bizot *et al.*, *Phys. Lett.* **86B**, 395 (1979).
- [23] M. Castellano, G. Di Giugno, J. Humphrey, E. Sassi Palmieri, G. Troise, U. Troya, and S. Vitale, *Nuovo Cimento Soc. Ital. Fis.* **14A**, 1 (1973).
- [24] G. Bardin, G. Burgun, R. Calabrese, G. Capon, R. Carlin *et al.*, *Nucl. Phys.* **B411**, 3 (1994).
- [25] G. Bardin, G. Burgun, R. Calabrese, G. Capon, R. Carlin *et al.*, *Phys. Lett. B* **255**, 149 (1991).
- [26] G. Bardin, G. Burgun, R. Calabrese, G. Capon, R. Carlin *et al.*, *Phys. Lett. B* **257**, 514 (1991).
- [27] T. Armstrong *et al.* (E760 Collaboration), *Phys. Rev. Lett.* **70**, 1212 (1993).

- [28] M. Ambrogiani *et al.* (E835 Collaboration), *Phys. Rev. D* **60**, 032002 (1999).
- [29] M. Andreotti, S. Bagnasco, W. Baldini, D. Bettoni, G. Borreani *et al.*, *Phys. Lett. B* **559**, 20 (2003).
- [30] V. Punjabi, C. Perdrisat, K. Aniol, F. Baker, J. Berthot *et al.*, *Phys. Rev. C* **71**, 055202 (2005).
- [31] O. Gayou *et al.* (Jefferson Lab Hall A Collaboration), *Phys. Rev. Lett.* **88**, 092301 (2002).
- [32] O. Gayou, K. Wijesooriya, A. Afanasev, M. Amarian, K. Aniol *et al.*, *Phys. Rev. C* **64**, 038202 (2001).
- [33] A. Puckett, E. Brash, M. Jones, W. Luo, M. Mezziane *et al.*, *Phys. Rev. Lett.* **104**, 242301 (2010).
- [34] R. Madey *et al.* (E93-038 Collaboration), *Phys. Rev. Lett.* **91**, 122002 (2003).
- [35] E. Geis *et al.* (BLAST Collaboration), *Phys. Rev. Lett.* **101**, 042501 (2008).
- [36] L. Andivahis, P. E. Bosted, A. Lung, L. Stuart, J. Alster *et al.*, *Phys. Rev. D* **50**, 5491 (1994).
- [37] T. Pospischil *et al.* (A1 Collaboration), *Eur. Phys. J. A* **12**, 125 (2001).
- [38] H. Czyz, A. Grzelinska, J. H. Kuhn, and G. Rodrigo, *Eur. Phys. J. C* **33**, 333 (2004).
- [39] H. Czyz, A. Grzelinska, J. H. Kuhn, and G. Rodrigo, *Eur. Phys. J. C* **39**, 411 (2005).
- [40] S. Binner, J. H. Kuhn, and K. Melnikov, *Phys. Lett. B* **459**, 279 (1999).
- [41] H. Czyz, A. Grzelinska, and J. H. Kuhn, *Phys. Lett. B* **611**, 116 (2005).
- [42] H. Czyz, M. Gunia, and J. Kuhn, *J. High Energy Phys.* **08** (2013) 110.
- [43] <http://ific.uv.es/~rodrigo/phokhara/>.